JCTC Journal of Chemical Theory and Computation

Article

pubs.acs.org/JCTC

# Stochastic Dynamics with Correct Sampling for Constrained Systems

E. A. J. F. Peters,*[,†] N. Goga,[‡] and H. J. C. Berendsen[‡]

[†]Department of Chemical Engineering and Chemistry, Eindhoven University of Technology, P.O. Box 513, 5600 MB, Eindhoven, The Netherlands

[‡]Groningen Biomolecular Sciences and Biotechnology Institute and Zernike Institute for Advanced Materials, University of Groningen, Nijenborgh 7, 9747 AG, Groningen, The Netherlands

**ABSTRACT:** In this paper we discuss thermostatting using stochastic methods for molecular simulations where constraints are present. For so-called impulsive thermostats, like the Andersen thermostat, the equilibrium temperature will differ significantly from the imposed temperature when a limited number of particles are picked and constraints are applied. We analyze this problem and give two rigorous solutions for it. A correct general treatment of impulsive stochastic thermostatting, including pairwise dissipative particle dynamics and stochastic forcing in the presence of constraints, is given and it is shown that the constrained canonical distribution is sampled rigorously. We discuss implementation issues such as second order Trotter expansions. The method is shown to rigorously maintain the correct temperature for the case of extended simple point charge (SPC/E) water simulations.

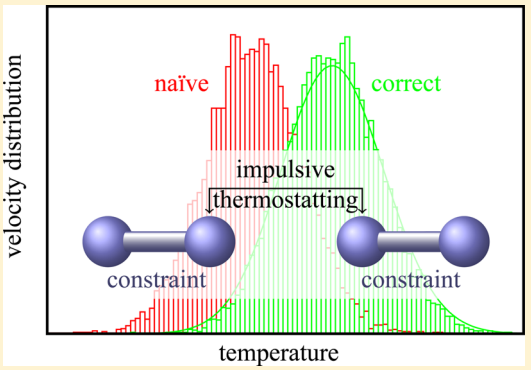


## 1. INTRODUCTION

Stochastic methods have a long history in molecular dynamics simulations.[1−4] They are used to mimick the nonconservative forces exerted by degrees of freedom that are not explicitly represented in a simplified molecular dynamics (MD) force field. The conservative forces are taken care of by constructing potentials of mean force. The nonconservative forces form a combination of velocity-dependent frictional forces and random components with prescribed correlation in time and space, leading to the *generalized Langevin equation*. The inclusion of correlation in time—while not impossible[1]—brings considerable additional complications and has not found widespread use. Therefore, we restrict our considerations to random components with white noise character. We allow different friction coefficients for different particles and explicitly allow such combinations of frictions that the resulting dynamics is Galilean-invariant, a requirement for the dynamics to obey the Navier−Stokes relations in the macroscopic limit.

While stochastic dynamics was originally designed to faithfully reproduce the dynamics of complex systems with simplified descriptions, its applications have extended to achieve efficient sampling of phase space irrespective of the faithfulness of the generated dynamics. Thus, in *coarse-grained dynamics* using superatoms, the phase space sampling will in general be faster without or with reduced stochastic terms. In such systems the inclusion of weak stochastic terms will act as a *thermostat*. It is mandatory that the velocity changes by friction and noise correctly sample a canonical velocity distribution.

Many algorithmic implementations of stochastic dynamics involve integration of the stochastic equations of motion over a time step: the influence of friction and noise can be incorporated within the accuracy of the (velocity-)Verlet or leapfrog algorithms.[5−7] Such algorithms tend to become rather complex and simplified forms have been devised.

There is also a second class of stochastic thermostats often used in MD that do not attempt to numerically solve a stochastic differential equation. Examples of such methods are the Andersen[8] and the Lowe−Andersen[9] thermostat. In Andersen's method, after performing reversible dynamics driven by the conservative interactions using, for example, a Verlet algorithm, particles are picked and their velocity is reset by drawing a new velocity from the proper Maxwell−Boltzmann distribution. In the Lowe method the same thing is done for the relative velocity of pairs of particles located within a certain cutoff radius from each other. These methods sample the Maxwell−Boltzmann distribution exactly, while having a less well-defined dynamics.

One can also pick a set of particles or pairs and only partially reset their velocities. In this way an updated velocity is a weighted average of the old value and a random variable. This kind of updating can be performed in such a way that it is a valid discretization of a stochastic differential equation, that is, for $\Delta t \rightarrow 0$ the Langevin equation is recovered. But, in addition, also for finite time steps the Maxwell−Boltzmann distribution is sampled exactly. This approach has been advocated in recent publications.[10−12]

We will denote the procedure of picking individual or pairs of particles and (partially) resetting their velocities as *impulsive* application of friction and noise. This kind of thermostatting has a large flexibility. One can try to discretize underlying stochastic differential equations faithfully, such as in the case of

**Received:** May 1, 2014

   dx.doi.org/10.1021/ct500380x | *J. Chem. Theory Comput.* XXXX, XXX, XXX−XXX

dissipative particle dynamics (DPD).[10,13] Alternatively, one might be concerned with effective thermalization while not detrimentally influencing the performance of the MD simulation. In this case one can apply, for example, the Lowe thermostat or the impulsive thermostats advocated by Goga et al.[11]

The Andersen thermostat has been widely used and the more novel impulsive thermostats are gaining popularity. In this article we consider the application of these thermostats in the presence of holonomic constraints. It was proven by Ryckaert and Ciccotti[14] that when applying the Andersen thermostat to *all* particles and subsequently applying constraints, the correct velocity distribution is sampled. However, one of the nice features of the nonconstrained Andersen/Lowe thermostat is that one also can pick one particle or a pair or a limited number of particles and rethermalize only these. It turns out that in the presence of constraints, this procedure leads to erroneous results.

We find that, when naïvely applying the impulsive thermostats to a subset of all particles, as in a nonconstrained case, and subsequently projecting the velocities according to the imposed constraints, an incorrect velocity distribution is sampled. This can lead to serious deviations of the temperature from the one that one would like to be imposed by the thermostat. This is a not widely acknowledged issue and therefore worthwhile pointing out. We will not only focus attention on this problem but also provide a solution for it.

This paper is focused on the handling of constraints for impulsive thermostats. In comparison, for deterministic thermostats (such as Nosé–Hoover) constraints do not impose extra complications, and methods of rigorously handling them are well-known. For constrained Langevin dynamics, however, some proposals in literature have been published.[15,16] These include second-order schemes, but no schemes that leave the Boltzmann distribution invariant, as an impulsive thermostat does. Most of these papers mainly contain theoretical derivations base on the numerical approximations for stochastic differential equations (SDEs). These papers consider the "simple" Langevin dynamics with a constant friction factor, where the frictional force on a particle is proportional to its velocity. Our method is related, because it can be used for the numerical solution of constrained Langevin equations. However, our method is more general because it also considers a system with dissipative Galilean-invariant pair interactions (DPD) and can be used for impulsive thermostats that are not formulated in terms of an SDE (Andersen and Lowe–Andersen).

This article is organized as follows. After recapitulating the theory[10−12] for impulsive thermostatting in unconstrained systems (Section 2), we show two examples where naïve application of this theory to constrained systems leads to an equilibrium temperature that deviates from the reference temperature imposed by the thermostat (Section 3). In Section 4 we present a formalism for impulsive thermostatting, based on a consistent matrix notation. This includes (in Section 4.2) the projection operator that realizes the projection of unconstrained velocities onto the constrained hypersurface. After stating the constrained canonical distribution of Cartesian velocities in Section 4.3, we present the correct handling of impulsive thermostatting in the presence of constraints in Section 4.4. This is the main result of this paper.

Section 5 discusses the full integration of the equations of motion, including velocity updates by friction and noise and the possibility of Trotter operator splitting. In Section 6 we show that application of the proper thermostatting proposed in Section 4.4 to the examples of Section 2 yields correct results, as does a DPD-type thermostatting for rigid extended simple point charge (SPC/E) water using one pair per particle, independent of the strength of the applied friction. Finally, conclusions are discussed in Section 7.

## 2. IMPULSIVE THERMOSTATTING FOR UNCONSTRAINED SYSTEMS

Impulsive application of friction and noise to a single particle $i$ consists of a velocity reduction (or damping) of the particle, followed by a partial rethermalization to the canonical (Maxwell–Boltzmann) distribution. We assume an isotropic application in three dimensions, although this is not a requirement.

Denoting the "old" velocity vector by $\mathbf{v}_i$, and a vector of three independent Gaussian stochastic variables of zero mean and variance 1 by $\boldsymbol{\xi}$, the new velocity $\mathbf{v}_i'$ is given by

$$\mathbf{v}_i' = (1 - f)\mathbf{v}_i + g\boldsymbol{\xi} \tag{1}$$

$$\langle m_i \mathbf{v}_i'^2 \rangle = (1 - f)^2 \langle m_i \mathbf{v}_i^2 \rangle + 3m_i g^2 \tag{2}$$

Requiring that the kinetic energy obeys the correct equipartition value corresponding to the temperature of the heat bath, $\langle m_i \mathbf{v}_i^2 \rangle = \langle m_i \mathbf{v}_i'^2 \rangle = 3k_B T$, gives

$$g^2 = f(2 - f)k_B T/m_i \tag{3}$$

Note that a sum of Gaussian variables gives again a Gaussian variable. Therefore, the stationary distribution is Gaussian with the correct variance, that is, the proper Maxwell–Boltzmann distribution.

When explicitly integrating over a finite time-step $\Delta t$, the stochastic differential equation corresponding to Langevin dynamics with constant friction:

$$m_i \mathrm{d}\mathbf{v}_i = -\zeta \mathbf{v}_i \mathrm{d}t + \sqrt{2k_B T\zeta}\, \mathrm{d}\mathbf{W}_t \tag{4}$$

where $\mathbf{W}_t$ is a three-dimensional Wiener process, one finds that the exact so-called weak solution is given by eq 1 with $f = 1 - \exp(-\zeta \Delta t/m_i)$ and $g^2 = (k_B T/m_i)[1 - \exp(-2\zeta \Delta t/m_i)]$. This is an example that obeys relation eq 3.

This scheme can straight-forwardly be generalized[11] to re-equilibrating relative velocities $\mathbf{v}_{ij} = \mathbf{v}_i - \mathbf{v}_j$, by the substitution $\mathbf{v}_i \rightarrow \mathbf{v}_{ij}$ and $m_i \rightarrow \mu_{ij}$ (reduced mass). In this case the equipartition theorem tells that $\mu_{ij}\mathbf{v}_{ij}^2 = 3k_B T$, with $\mu_{ij}^{-1} = m_i^{-1} + m_j^{-1}$. For pairs of particles the thermostatting should leave the center-of-mass velocity (or the total momentum) invariant, such that

$$\mathbf{v}_i' = \mathbf{v}_i + (\mu_{ij}/m_i)(\mathbf{v}_{ij}' - \mathbf{v}_{ij}),\ \mathbf{v}_j' = \mathbf{v}_j - (\mu_{ij}/m_j)(\mathbf{v}_{ij}' - \mathbf{v}_{ij}) \tag{5}$$

This implementation is named[11] isotropic, since the directions of applied noise are isotropically distributed in three dimensions.

One may also apply the friction and fluctuating force only in the direction of the connecting vector (indicated by unit vector $\hat{\mathbf{r}}_{ij}$). In this case we get a one-dimensional *parallel* update of the relative velocity, equivalent to the friction and noise proposed in the original DPD method:[17]

$$\mathbf{v}_{ij}' = \mathbf{v}_{ij} - f(\mathbf{v}_{ij} \cdot \hat{\mathbf{r}}_{ij})\hat{\mathbf{r}}_{ij} + g\hat{\mathbf{r}}_{ij}\xi \tag{6}$$


dx.doi.org/10.1021/ct500380x | J. Chem. Theory Comput. XXXX, XXX, XXX−XXX

Also here we find the requirement that $g^2 = f\,(2 - f)k_BT/\mu_{ij}$. Similarly, a two-dimensional *perpendicular* scheme can be devised with velocity update in the plane perpendicular to $\hat{\mathbf{r}}_{ij}$. We refer to Section 4.1 for a more formal description and to ref 11 for explicit algorithms in these cases.

## 3. TWO EXAMPLES OF NAÏVE IMPLEMENTATIONS OF CONSTRAINTS

In the absence of constraints the equations given above guarantee that the application of friction and noise to individual particles or particle pairs drives the actual temperature of the affected degrees of freedom toward the reference temperature. Because of kinetic energy transfer resulting from interparticle forces (thermal conduction) the temperature of the system as a whole will tend to the reference temperature; hence, such friction and noise acts as a thermostat.

In the presence of constraints this is not the whole story. After applying friction and noise according to the equations given above, the velocities will not be constrained and contain components in directions deviating from the constraint hypersurface. In practice a *constraint step* is introduced, which corrects these deviations. While Ryckaert and Ciccotti[14] have proven that a correct canonical ensemble for the constrained system is obtained after applying a constraint algorithm to a system in which *all* degrees of freedom are completely randomized to a Maxwellian velocity distribution, it is not at all clear that applying (partial) thermostatting constraints to selected degrees of freedom yields correct temperatures if constraints are present. In fact, it is clear from studying two simple examples that this is *not* the case and that noticeable errors in thermal behavior result.

Consider a one-dimensional system of homonuclear diatomic molecules. Each atom has mass $m$; the molecular mass is $2m$. Consider one particular molecule with atoms 1 and 2 and apply thermostatting to atom 1. This situation is depicted in Figure 1.

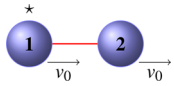


**Figure 1.** Thermostatting a one-dimensional system of homonuclear diatomic molecule. One atom indicated by the star is naïvely thermostated. After imposing the bond-length constraint the kinetic temperature has a different value from the imposed heat-bath temperature.

The molecule (and thus each of the atoms) has an initial velocity $v_0$. Now apply friction and noise to atom 1, yielding velocities $v_1'$ and $v_2'$:

$$v_1' = (1 - f)v_0 + g\xi;\; v_2' = v_0 \tag{7}$$

where $g$ follows from eq 3. Now apply constraints: in this simple case the constraints remove the relative velocity, and the new constrained velocities are equal for both atoms and equal to the center-of-mass velocity

$$v_{cm} = \frac{1}{2}(v_1' + v_2') = v_0 - \frac{1}{2}fv_0 + \frac{1}{2}g\xi \tag{8}$$

The new mean-squared velocities are equal to

$$\langle v_{cm}^2\rangle = \left(1 - \frac{1}{2}f\right)^2\langle v_0^2\rangle + \frac{1}{4}g^2 = \left(1 - \frac{1}{2}f\right)^2\langle v_0^2\rangle + \frac{1}{4}f(2 - f)\frac{k_BT}{m} \tag{9}$$

We now look for the equilibrium kinetic temperature $T_{kin}$ that the system will attain and for which

$$\langle v_{cm}^2\rangle = \langle v_0^2\rangle = \frac{k_BT_{kin}}{2m} \tag{10}$$

Using eqs 9 and 10 we find

$$T_{kin} = \frac{1 - \frac{1}{2}f}{1 - \frac{1}{4}f}T \tag{11}$$

The equilibrium kinetic temperature is smaller than the reference temperature of the heat bath. Thus, the constraint algorithm does not properly remove the excess velocity generated by friction and noise outside the constraint hypersurface. In the case of full randomization of the first atom ($f = 1$), the equilibrium temperature is only 2/3 of the reference temperature. This is an example of an Andersen thermostat applied to a subset of particles in the presence of constraints.

As a second example consider a one-dimensional system of homonuclear diatomic molecules. Each atom has mass $m$, so the molecular mass is $2m$. Consider two neighboring molecules $A$ and $B$ with atoms 1 and 2 and, respectively, 3 and 4. Apply DPD friction and noise to particle pair 2−3, see Figure 2.

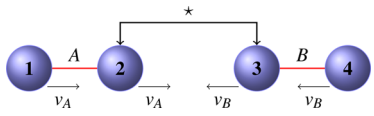


**Figure 2.** Two one-dimensional homonuclear diatomic molecules with bond-length constraints. A pairwise impulsive thermostatting is applied to the particles 2−3.

Molecule $A$ (and thus each of the atoms 1 and 2) has an initial velocity $v_A$. Likewise molecule $B$ with atoms 3 and 4 has velocity $v_B$. Now apply friction and noise to the pair 2−3 according to the equations given in Section 2. The velocity difference $v_{AB} = v_A - v_B$ is modified to

$$v_{AB}' = (1 - f)v_{AB} + g\xi \tag{12}$$

where the mass that should be used to compute $g$ in eq 3 is the reduced mass $\mu_{AB} = m/2$.

The resulting velocity difference is then distributed equally between atoms 2 and 3 such that the center-of-mass of 2 + 3 is not influenced, yielding

$$\begin{aligned} v_2' &= \left(1 - \frac{1}{2}f\right)v_A + \frac{1}{2}fv_B + \frac{1}{2}g\xi \\ v_3' &= \left(1 - \frac{1}{2}f\right)v_B + \frac{1}{2}fv_A - \frac{1}{2}g\xi \end{aligned} \tag{13}$$

The next step is application of the constraints, that is, constructing the center-of-mass velocity of the molecules:


dx.doi.org/10.1021/ct500380x | J. Chem. Theory Comput. XXXX, XXX, XXX−XXX

$$v'_A = \frac{1}{2}(v_A + v'_2) = \left(1 - \frac{1}{4}f\right)v_A + \frac{1}{4}fv_B + \frac{1}{4}g\xi$$
$$v'_B = \frac{1}{2}(v'_3 + v_B) = \left(1 - \frac{1}{4}f\right)v_B + \frac{1}{4}fv_A - \frac{1}{4}g\xi \quad (14)$$

If we evaluate the second moments this gives

$$\langle v_A^2\rangle' = \left(1 - \frac{1}{4}f\right)^2\langle v_A^2\rangle + \frac{1}{16}f^2\langle v_B^2\rangle + \frac{1}{2}f\left(1 - \frac{1}{4}f\right)\langle v_A v_B\rangle + \frac{1}{16}g^2$$
$$\langle v_A v_B\rangle' = \frac{1}{4}f\left(1 - \frac{1}{4}f\right)(\langle v_A^2\rangle + \langle v_B^2\rangle) + \left[\left(1 - \frac{1}{4}f\right)^2 + \frac{1}{16}f^2\right]\langle v_A v_B\rangle - \frac{1}{16}g^2 \quad (15)$$

where the equation for $\langle {v_B}^2\rangle'$ is the same of that of $\langle {v_A}^2\rangle'$ with indices $A$ and $B$ interchanged. If the thermostat is applied multiple times finally a fixed point is reached for the Gaussian velocity distribution with $\langle {v_A}^2\rangle' = \langle {v_B}^2\rangle' = \langle {v_A}^2\rangle' = \langle {v_B}^2\rangle'$ and $\langle v_A v_B\rangle' = \langle v_A v_B\rangle$. This gives,

$$\langle v_A^2\rangle = \frac{g^2}{8f\left(1 - \frac{1}{4}f\right)} = \frac{1 - \frac{1}{2}f}{1 - \frac{1}{4}f}\frac{k_B T}{2m};\ \langle v_A v_B\rangle = 0 \quad (16)$$

such that

$$T_{kin} = \frac{1 - \frac{1}{2}f}{1 - \frac{1}{4}f}T \quad (17)$$

As in the Langevin case the equilibrium temperature is lower than the reference temperature, especially if $f$ deviates significantly from 0.

The main conclusion is that a naïve implementation of impulsive thermostats such as the Andersen, Lowe–Andersen, DPD thermostat of Peters, or the family of thermostats proposed by Goga et al. will, if constraints are present, give rise to a systematic deviation of the computed kinetic temperature from the imposed heat-bath temperature. How serious this deviation is depends on the magnitude of $f$ and on the sequence of thermostatting operations followed by the application of constraints.

## 4. FORMALISM FOR IMPULSIVE THERMOSTATTING

In this section we will formally describe impulsive thermostatting using matrix notation. The central point is the velocity correlation matrix that follows from the equipartition theorem of statistical mechanics; the thermostatting must preserve its canonical form. We first describe the rather obvious *unconstrained case*, where we introduce a "primitive thermostatting operation" involving a one-dimensional velocity update, and analyze when a sequence of operations requires sequential application and when it can be allowed to be applied in parallel. Then we consider the *constrained case*, first describing the action of constraint routines using a similar matrix notation, followed by a formulation of the canonical equipartition in a constrained system.

**4.1. The Unconstrained Case.** Before discussing our solution to the problem of correct thermostatting in the presence of constraints we will introduce a more general notation for the thermostats introduced in Section 2.

In this paper we are interested in expressing equations using Cartesian coordinates. There are $n$ particles, $i = 1\cdots n$, and we will assume three spatial coordinates although this is not essential. To present the results in their full generality we will adopt the following matrix notation:

1. $\mathbf{x}$ is a $3n$ dimensional 1-column matrix representing the 3n coordinates of $\mathbf{r}_i$, $i = 1\cdots n$.
2. $\mathbf{v}$ is a $3n$ dimensional 1-column matrix representing the 3n coordinates of $\dot{\mathbf{r}}_i$, $i = 1\cdots n$.
3. $\mathbf{M}$ is a $3n \times 3n$ square matrix with $m_1$, $m_1$, $m_1$, $m_2$, $m_2$, $m_2$, ..., $m_n$, $m_n$, $m_n$ along its diagonal.

We will consider the following thermostatting operation:

$$\mathbf{v}' = (\mathbf{I} - \mathbf{F})\mathbf{v} + \mathbf{G}\boldsymbol{\xi} \quad (18)$$

where $\boldsymbol{\xi}$ is a column vector with normally distributed random numbers with mean 0 and covariance matrix $\mathbf{I}$. Here the matrices $\mathbf{F}$ and $\mathbf{G}$ do not depend on $\mathbf{v}$.

The equilibrium distribution of velocities is the Maxwell–Boltzmann distribution. This is a Gaussian distribution with covariance matrix

$$\langle \mathbf{v}\mathbf{v}^T\rangle = k_B T\mathbf{M}^{-1} \quad (19)$$

Since adding Gaussian variables results in a stochastic variable that is itself normally distributed, also $\mathbf{v}'$ as computed by eq 18 is a Gaussian variable. This means that is is fully specified by its covariance matrix (and its mean). The thermostat has the Maxwell–Boltzmann distribution as invariant distribution if the covariance matrix of $\mathbf{v}'$ is also given by eq 19. This implies a relation between $\mathbf{F}$ and $\mathbf{G}$, namely,

$$k_B T\mathbf{M}^{-1} = (\mathbf{I} - \mathbf{F})k_B T\mathbf{M}^{-1}(\mathbf{I} - \mathbf{F}^T) + \mathbf{G}\mathbf{G}^T$$
$$\mathbf{G}\mathbf{G}^T = k_B T(\mathbf{F}\mathbf{M}^{-1} + \mathbf{M}^{-1}\mathbf{F}^T - \mathbf{F}\mathbf{M}^{-1}\mathbf{F}^T) \quad (20)$$

This relation can be easily solved for $\mathbf{G}$ if, for example, $\mathbf{F}$ and $\mathbf{M}^{-1}$ are diagonal matrices. This is the case in simple Langevin dynamics. But in other case, expecially DPD and the Lowe–Andersen thermostat, where pair-interactions are considered $\mathbf{F}$ is nondiagonal. In principle, $\mathbf{G}$ can always be found by applying Cholesky decomposition. This is, however, computationally very expensive.

The relation can, however, be easily obeyed if $\mathbf{G}$ is a one-dimensional column vector, such that $\boldsymbol{\xi}$ is in fact a single random number, and $\mathbf{F}$ is a square matrix of rank one. We will name this case where only one random number is needed a *primitive thermostatting operation*. Instead of using a matrix $\mathbf{G}$ with a rank bigger than 1 we will use a sequence of primitive thermostatting operations where each $\mathbf{G}$ is a $3n \times 1$ matrix, that is, a column vector. We will denote such a column vector at step $k$ in the sequence of primitive thermostatting operations as $\mathbf{g}_k$, such that

$$\mathbf{v}_{k+1} = (\mathbf{I} - \mathbf{F}_k)\mathbf{v}_k + \mathbf{g}_k\xi_k \quad (21)$$

Let us perform, say $m$ number of these operations, then: $\mathbf{v}_0 \equiv \mathbf{v}$ and $\mathbf{v}' \equiv \mathbf{v}_m$. To make sure that each of these operations leaves the unconstrained Maxwell–Boltzmann distribution invariant we require that, according to eq 20,

$$\mathbf{g}_k\mathbf{g}_k^T = k_B T[\mathbf{F}_k\mathbf{M}^{-1} + \mathbf{M}^{-1}\mathbf{F}_k^T - \mathbf{F}_k\mathbf{M}^{-1}\mathbf{F}_k^T] \quad (22)$$


dx.doi.org/10.1021/ct500380x | J. Chem. Theory Comput. XXXX, XXX, XXX–XXX

which can be used to check or construct specific forms of valid primitive thermostatting operations.

For example, a simple Langevin damping on one Cartesian degree of freedom (which we can number 1 without loss of generality) yields a matrix $\mathbf{F}_k$ with one value $\mathbf{F}_{11} = f_k$ and zero otherwise; application of eq 22 immediately shows that $\mathbf{g}_k$ is a vector with one component $g_1$, with $g_1^2 = (k_B T/m_1)(2f - f^2)$. A less trivial example is the *iso*-DPD variant, see eq 5, which—for one Cartesian component numbered 1 for particle $i$ and 2 for particle $j$—reads

$$\begin{aligned} v_1' &= v_1 + \frac{\mu}{m_1}[(1-f)(v_1 - v_2) + g\xi] \\ v_2' &= v_2 - \frac{\mu}{m_2}[(1-f)(v_1 - v_2) + g\xi] \end{aligned} \tag{23}$$

with $g^2 = f(2-f)k_B T/\mu$. In matrix notation this is equivalent to eq 21 with

$$\mathbf{F} = \mu f \mathbf{M}^{-1}\begin{pmatrix} 1 & -1 \\ -1 & 1 \end{pmatrix};\ \mathbf{g} = g\mu\mathbf{M}^{-1}\begin{pmatrix} 1 \\ -1 \end{pmatrix} \tag{24}$$

which fulfills eq 22.

More generally, requirement eq 22 is obeyed for

$$\mathbf{F}_k = f_k \frac{\mathbf{g}_k \mathbf{g}_k^T \mathbf{M}}{\mathbf{g}_k^T \mathbf{M} \mathbf{g}_k},\ \text{where } \mathbf{g}_k^T \mathbf{M} \mathbf{g}_k = f_k(2 - f_k)k_B T \tag{25}$$

which can be confirmed by back-substitution. It is easily verified that $\mathbf{F}$ and $\mathbf{g}$ of the iso-DPD example given above in eq 24, fulfill eq 25.

If the primitive thermostatting operations are carried out sequentially, the Maxwell−Boltzmann distribution is preserved throughout the sequence. Sequential operation means that each operation is completed (both damping and noise have been applied) before the next operation starts; parallel operation means that the damping is applied to all involved particles, after which the total noise is added. Sequential operation is not needed in all cases; if each particle is touched only once, the primitive operations commute with each other and can be carried out in parallel as well.

This special case occurs if all the vectors $\mathbf{g}_k$ obey the orthogonality relation $\mathbf{g}_k^T \mathbf{M} \mathbf{g}_l = 0$ for all $l \neq k$; then also $\mathbf{F}_k\, \mathbf{F}_l = \mathbf{0}$. This orthogonality condition is, for example, obeyed if the entry in $\mathbf{g}_k$ for a specific particle index is nonzero only for one $k$-value (or never), that is, as each velocity coordinate is touched by the thermostat not more than once. This is commonly the case in Andersen and Langevin types of thermostats where individual particles are thermostated.

In the case the orthogonality conditions hold we can define an overall

$$\mathbf{F} = \sum_k \mathbf{F}_k \text{ and } \mathbf{G} = [\mathbf{g}_1, \mathbf{g}_2, \cdots] \tag{26}$$

Now the primitive thermostatting operations commute and the thermostatting need not be applied sequentially but can be applied in parallel. If the orthogonality condition is not obeyed it is hard to give explicit forms of $\mathbf{F}$ and $\mathbf{G}$ as used in eq 18. In practice no explicit form is created or needed, but the primitive thermostat operations are performed sequentially such as indicated in eq 21.

A second special case is when we consider the infinitesimal case $f_k \to \nu_k \mathrm{d}t$. In this case we find (in sloppy notation) that

$$\begin{aligned} \mathbf{F}_k &= (\nu_k \mathrm{d}t)\mathbf{M}^{-1}\mathbf{u}_k\mathbf{u}_k^T \text{ and } \mathbf{g}_k \\ &= \sqrt{2k_B T \nu_k \mathrm{d}t}\,\mathbf{M}^{-1}\mathbf{u}_k, \text{ with } \mathbf{u}_k^T\mathbf{M}^{-1}\mathbf{u}_k \\ &= 1. \end{aligned} \tag{27}$$

here the direction vector, $\mathbf{u}_k$, is normalized by using the inverse mass-matrix as "metric". In the infinitesimal limit the result will be independent of the sequence of primitive operations, So, in this infinitesimal case eq 26 holds. Clearly, this additivity can break down when going to finite time steps.

In a more formal mathematical treatment the combination of time-step and Gaussian, $(\mathrm{d}t)^{1/2}\xi_k$, will be denoted as an infinitesimal increment of the Wiener process $\mathrm{d}W_k$. In this case we get

$$\mathbf{M}\mathrm{d}\mathbf{v}_k = -\nu_k \mathbf{u}_k \mathbf{u}_k^T \mathbf{v}_k \mathrm{d}t + \sqrt{2k_B T \nu_k}\,\mathbf{u}_k \mathrm{d}W_k \tag{28}$$

The time integration over a finite time-step, $\Delta t$, in this case gives explicit expressions for $\mathbf{F}_k$ and $\mathbf{g}_k$, as

$$\begin{aligned} \mathbf{F}_k &= (1 - \exp(-\nu_k \Delta t))\mathbf{M}^{-1}\mathbf{u}_k\mathbf{u}_k^T \text{and} \mathbf{g}_k \\ &= \sqrt{k_B T(1 - \exp(-2\nu_k \Delta t))}\,\mathbf{M}^{-1}\mathbf{u}_k \end{aligned} \tag{29}$$

which obey relation eq 25, as expected. Note that these individual primitive operations for finite time steps need to be applied sequentially and not in parallel. In parallel applications eq 26 would be used, but in this case eq 25 is not obeyed (unless the orthogonality condition holds for the $\mathbf{u}_k$ values).

In the case of DPD or Langevin dynamics the reasoning runs in the opposite direction. There is a stochastic differential equation that needs to be integrated. Now, one can split this equation into primitive parts. Then sequentially a discrete finite time-step approximation for each part is made, and they are applied sequentially. This is usually called an operator-splitting scheme.[13,18] If each part obeys the correct fluctuation−dissipation relation eq 25, then sequential application as in eq 18 yields an invariant Maxwell−Boltzmann distribution. Even though an approximation of the dynamics is used, the equilibrium properties are fully correct. For example, Peters[10] proposed two possible forms for $\mathbf{F}_k$ for the DPD case, of which one corresponds to eq 29.

For Lowe−Andersen and DPD type thermostats pairs of particles are thermostated and commonly a specific particle participates in multiple pairs. Therefore, in this case, the sequential application is essential. For pairwise interactions one usually requires that the total momentum is conserved. The requirement gives that $\sum_i'[\mathbf{M}\mathbf{g}_k]_i = 0$, where the primed-sum indicates the sum over all indices corresponding to one direction, that is, $x$, $y$, or $z$. A straightforward way to establish this for pairwise interaction is to rewrite $\mathbf{g}_k = \mathbf{M}^{-1}\mathbf{h}_k$, where for the two particle-coordinate indices $i$ and $j$: $h_{k,i} = -h_{k,j}$, while $h_{k,m} = 0$ for $m \neq i,j$. The example given in eq 24 is of this form.

Note that if one considers the three independent directions $x$, $y$, and $z$ sequentially, then the orthogonality condition discussed before is obeyed. Also if we consider orthogonal directions, for example, into the direction $\hat{\mathbf{r}}_{ij}$ and the directions perpendicular to that, this is the case. Therefore, for a pair of particles the three directions can be handled in parallel. The pairwise schemes discussed before have this required form.

The pairwise form is a way to introduce conservation of linear momentum, or Galilean invariance, into the thermostatting. One might wonder how to (locally) conserve angular momentum. Angular momentum is conserved always when


dx.doi.org/10.1021/ct500380x | J. Chem. Theory Comput. XXXX, XXX, XXX−XXX

pairwise forces are applied along the connecting vector. This means it is valid for the original parallel form of DPD, but not when also perpendicular forces are considered, such as in the isotropic or perpendicular DPD implementations.

**4.2. Velocity Constraining Expressed as Projection Matrix.** We now turn to constrained systems and describe how velocities are constrained by a projection method.

Consider a system of $n$ particles with $n_c$ holonomic constraints, given by

$$\sigma_s(\mathbf{r}_1, ..., \mathbf{r}_n) = \sigma_s(\mathbf{x}) = 0 \text{ for } s = 1, ..., n_c \tag{30}$$

These equations define a *constraint manifold*, a $(3N - n_c)$-dimensional subspace $\mathcal{J}$, to which the coordinates are restricted at all times. The $n_c$ gradient vectors $\nabla\boldsymbol{\sigma}_s$ are perpendicular to $\mathcal{J}$ at a given reference point; they form a (nonorthogonal) basis spanning the vector space orthogonal to the hyperplane tangential to the constraint manifold. We define the *constraint matrix* $\mathbf{C}$ with components

$$C_{si} = \frac{\partial \sigma_s}{\partial x_i} \tag{31}$$

Now consider an arbitrary (unconstrained) vector $\mathbf{v}^u$ in $3n$-dimensional space. We wish to decompose $\mathbf{v}^u$ into a *projection* $\mathbf{v}^c = (\mathbf{I} - \mathbf{P})\mathbf{v}^u$ of $\mathbf{v}^u$ onto the constraint space $\mathcal{J}$ and a remainder $\mathbf{P}\mathbf{v}^u$, which is a vector perpendicular to the constraint hyperspace at the reference point. The vector $\mathbf{v}^u$ could represent the velocities of all particles and construction of the projection $\mathbf{v}^c = (\mathbf{I}-\mathbf{P})\mathbf{v}^u$ would remove components of the velocities that extend beyond $\mathcal{J}$. This implies that the vector $\mathbf{v}^c$ must be perpendicular to all gradient vectors

$$\mathbf{C}\mathbf{v}^c = \mathbf{0} \tag{32}$$

These equations are valid for any vector $\mathbf{v}$, but are in fact the constraint equations for velocities, derived from the fact that the time derivatives of the constraints, eq 30, are zero. Thus, the constrained velocities are subject to

$$\forall\ s\colon \dot{\sigma}_s(\mathbf{x}) = \sum_i \frac{\partial \sigma_s}{\partial x_i}\dot{x}_i = \sum_i C_{si} v_i^c = 0 \tag{33}$$

which is equivalent to eq 32.

The projection $(\mathbf{I} - \mathbf{P})$ is realized by a routine vconstr with two vectorial arguments

$$\mathbf{v}^c = (\mathbf{I} - \mathbf{P})\mathbf{v}^u = \text{vconstr}(\mathbf{v}^u; \mathbf{x}^{ref}) \tag{34}$$

The implementation[8,14] proceeds as follows, using $n_c$ Lagrange multipliers $\lambda_s$. Every velocity is projected onto the hyperplane tangent to the constraint manifold by

$$v_i^c = v_i^u - \frac{1}{m_i}\sum_s \lambda_s \frac{\partial \sigma_s}{\partial x_i} \tag{35}$$

Each velocity correction has a weight factor equal to the inverse mass of the corresponding particle. This ensures that the total momentum for the particles remains unchanged. Equation 35 reads in matrix notation:

$$\mathbf{v}^c = \mathbf{v}^u - \mathbf{M}^{-1}\mathbf{C}^T\boldsymbol{\lambda} \tag{36}$$

where $\boldsymbol{\lambda}$ is determined such that the constraint equations for velocities, eq 32, are satisfied. This implies that

$$\mathbf{C}\mathbf{v}^u = \mathbf{C}\mathbf{M}^{-1}\mathbf{C}^T\boldsymbol{\lambda} \tag{37}$$

Defining

$$\mathbf{Z} \overset{\text{def}}{=} \mathbf{C}\mathbf{M}^{-1}\mathbf{C}^T \tag{38}$$

it follows that

$$\boldsymbol{\lambda} = \mathbf{Z}^{-1}\mathbf{C}\mathbf{v}^u \tag{39}$$

Inserting eq 39 into eq 36, we obtain

$$\mathbf{v}^c = \mathbf{v}^u - \mathbf{M}^{-1}\mathbf{C}^T\mathbf{Z}^{-1}\mathbf{C}\mathbf{v}^u = (\mathbf{I} - \mathbf{P})\mathbf{v}^u \tag{40}$$

where

$$\mathbf{P} \overset{\text{def}}{=} \mathbf{M}^{-1}\mathbf{C}^T\mathbf{Z}^{-1}\mathbf{C} \tag{41}$$

This establishes that the routine vconstr will return the operation $(\mathbf{I} - \mathbf{P})$ applied to its first argument, to within a specified accuracy. The reference vector $\mathbf{x}^{ref}$ is the point on the constraint manifold at which the tangential projection plane is defined.

Note that $\mathbf{P}$, and hence also $\mathbf{I} - \mathbf{P}$, is a *projection matrix*, representing a projection operator. They are equal to their own squares, as is easily verified for $\mathbf{P}$ by using its definition eq 41.

While the *linear* projection operator $\mathbf{I} - \mathbf{P}$, as realized, for example, in RATTLE,[8] is all we need to constrain velocities, the integration of the equations of motion in discrete steps also requires a nonlinear projection of a coordinate displacement from a reference point onto the constraint hypersurface, as realized by SHAKE,[19] SETTLE,[20] and LINCS.[21,22] We shall denote this projection by xconstr:

$$\mathbf{x}^c = \text{xconstr}(\mathbf{x}^u; \mathbf{x}^{ref}) \tag{42}$$

Figure 3 visualizes the actions of vconstr and xconstr.

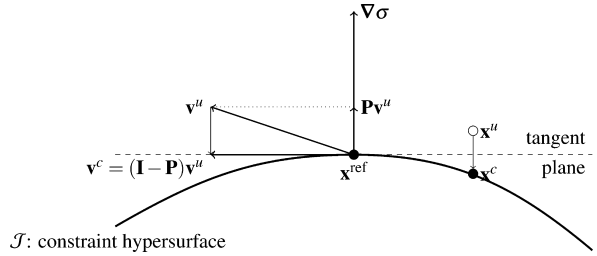


**Figure 3.** Constraint hypersurface $\mathcal{J}$: $\boldsymbol{\sigma} = 0$ and the actions of vconstr and xconstr: projection of a vector $\mathbf{v}^u$ onto the tangent plane to $\mathcal{J}$ at $\mathbf{x}^{ref}$ and projection of a point $\mathbf{x}^u$ onto $\mathcal{J}$ in the direction of the gradient to $\mathcal{J}$ at $\mathbf{x}^{ref}$.

**4.3. The Constrained Canonical Distribution.** To correctly resample velocities in the constrained case, we must first ask the question what the canonical distribution is for the constrained velocities. Ryckaert and Ciccotti[14] have shown that a set of unconstrained velocities sampled from a Maxwell–Boltzmann distribution, that is, a set of Gaussian variables with zero mean and correlation matrix given by eq 19, after applying velocity constraints according to eq 34, yields a set of velocities that are samples from the correct canonical probability distribution for constrained systems. This implies that the correlation matrix for constrained velocities is given by

$$\langle \mathbf{v}^c \mathbf{v}^{c,T} \rangle = k_B T(\mathbf{I} - \mathbf{P})\mathbf{M}^{-1} \tag{43}$$

This expression follows from working out the correlation matrix for $\mathbf{v}^c$:

$$\langle \mathbf{v}^c \mathbf{v}^{c,T} \rangle = k_B T(\mathbf{I} - \mathbf{P})\mathbf{M}^{-1}(\mathbf{I} - \mathbf{P}^T) \tag{44}$$

and using the relations


dx.doi.org/10.1021/ct500380x | J. Chem. Theory Comput. XXXX, XXX, XXX−XXX

$$\mathbf{P}\mathbf{M}^{-1} = \mathbf{M}^{-1}\mathbf{P}^T = \mathbf{P}\mathbf{M}^{-1}\mathbf{P}^T \tag{45}$$

which follow from the definitions of **P** eq 41 and **Z** eq 38. Equation 43 is the central theorem on which our paper is based.

Equation 43 suggests that the constrained Maxwell−Boltzmann velocity distribution can be generated as follows. First, generate $\mathbf{v}^u$ according to the Gaussian distribution corresponding to the covariance matrix of the unconstrained Maxwell−Boltzmann distribution. This is in practice simple because **M** is a diagonal matrix with the particle masses on the diagonal. Next, the unconstrained velocities can be constrained to the correct vector space by performing the projection eq 34: $\mathbf{v}^c = (\mathbf{I} - \mathbf{P})\mathbf{v}^u$.

**4.4. The Constrained Case.** The issue of correct thermostatting in the presence of contraints is to sample a Gaussian velocity distribution with covariance matrix given by eq 43. From the previous section we arrive at the conclusion that this can be done by first drawing random vectors from the unconstrained Maxwell−Boltzmann distribution and then constraining those vectors.

The problem with naïve implementations such as discussed in Section 3 is as follows. Suppose that for an initial system the velocities are distributed as they should be, that is, according to eq 43. Next, an unconstrained thermostat is applied. The resulting velocity distribution after that is not equal to the equilibrium unconstrained Maxwell−Boltzmann distribution, because there is still influence of the initial constrained velocity distribution. Neither will the distribution be the constrained one, because the thermostatting will not take the constraints into account. If subsequently the constraints are applied using eq 34, the resulting distribution is not equal to the correct constrained Maxwell−Boltzmann distribution.

An exception is the case where all particles are fully thermostated, for example, the Andersen thermostat applied to all particles. In that case, after the unconstrained thermostatting, we obtain the unconstrained Maxwell−Boltzmann distribution. When next applying the constrained we obtain the correct constrained velocity distribution (see Section 4.3)

Let us rephrase the main conclusion of the previous section: if we can make sure that we constrain an unconstrained Maxwell−Boltzmann distribution, we obtain the correct constrained one. So, a solution is to first construct an unconstrained Maxwell−Boltzmann distribution out of a constrained one. Next, perform thermostatting on the unconstrained velocities, and last, project these velocities onto the constrained space. We now have a valid thermostat for constrained systems.

We will now give our main result, namely, a simple method that does just that. Here it comes:

$$\mathbf{v}' = \mathbf{v} + \sqrt{k_B T}\,\mathbf{P}\mathbf{M}^{-1/2}\boldsymbol{\xi}_1 \tag{46}$$

$$\mathbf{v}'' = (\mathbf{I} - \mathbf{F})\mathbf{v}' + \mathbf{G}\boldsymbol{\xi}_2 \tag{47}$$

$$\mathbf{v}^{(\mathrm{new})} = (\mathbf{I} - \mathbf{P})\mathbf{v}'' \tag{48}$$

where $\boldsymbol{\xi}_1$ and $\boldsymbol{\xi}_2$ are two independent vectors of normally distributed variables with zero mean and unit variance. In this scheme the constrained canonical distribution is the invariant distribution.

The important new ingredient, compared to earlier schemes, is the first step. This step adds random components in the constrained directions such that the unconstrained Boltzmann distribution is recovered, if **v** is distributed according the constrained canonical distribution eq 43, because

$$\begin{aligned}\langle \mathbf{v}'\mathbf{v}'^T\rangle &= \langle \mathbf{v}\mathbf{v}^T\rangle + k_B T\mathbf{P}\mathbf{M}^{-1}\mathbf{P}^T \\ &= k_B T(\mathbf{I} - \mathbf{P})\mathbf{M}^{-1} + k_B T\mathbf{P}\mathbf{M}^{-1}\mathbf{P}^T \\ &= k_B T\mathbf{M}^{-1}\end{aligned} \tag{49}$$

In this derivation the properties of **P** as stated in eq 45 are used.

The second step, eq 47, is the usual thermostatting of unconstrained velocities. It usually consists of a sequence of primitive thermostatting events, which may be handled in parallel if the events are independent, as discussed in Section 4.1. The combined effect of eq 46 and eq 47 is that an unconstrained Maxwell−Boltzmann distribution is sampled (when the initial **v** sampled the constrained Maxwell−Boltzmann). So after these two steps we will have a re-equilibrated unconstrained Maxwell−Boltzmann velocity distribution. The last step, eq 48, which is an application of vconstr, performs the projection of the unconstrained velocities to the correct space. As shown in the previous section, projecting the unconstrained Maxwell−Boltzmann distribution in this way gives the correct constrained distribution.

Therefore, the algorithm correctly samples the constrained canonical distribution. If the initial velocity distribution is not the equilibrium one, then the second step, eq 47, causes the final distribution to approach this correct equilibrium distribution. The additional step, compared to previous implementations, is eq 46. This constitutes a generation of Gaussian numbers and a projection step only once per time step (and not once per primitive thermostatting event), which involves a very limited computational effort.

The new element is the reintroduction of vector components into the constrained directions. By the thermostatting these components are mixed in, also in the unconstrained directions. At the end the new velocities pointing into the constrained directions are projected out again. If the $f$ factors are small, say $O(\Delta t)$, the effect of this mixing in is also small and the major part of the perpendicular components that were introduced by eq 46 will be removed again by eq 48. In fact, in the infinitesimal limit the equations will reduce to the proper constrained Langevin or DPD equations.

In this scheme the thermostatting steps occur in the unconstrained velocity space. The reintroduction of the perpendicular components might feel somewhat artificial. One might wonder if it is not possible to fully remain inside the constrained space. In Appendix B we present such a scheme. However, we did not implement this scheme. The reason is that the scheme presented in the appendix needs many projection steps, that is, one or two for every primitive operation. Therefore, in general, it is much more expensive than the method presented in this section.

## 5. INTEGRATION OF THE EQUATIONS OF MOTION

Up to now we focused on the impulsive thermostatting. The impulsive thermostatting as introduced in this paper only changes velocities and leaves the positions unaltered. In an MD simulation this thermostatting needs to be combined with the "conservative part" of the equations of motion. A rigorous integration of the conservative equations of motion conserve energy and obeys, among other things, Liouville's theorem. This makes the classical Boltzmann distribution invariant under the conservative evolution.


dx.doi.org/10.1021/ct500380x | J. Chem. Theory Comput. XXXX, XXX, XXX−XXX

In practice the equations of motion are discretized. The finite time discretization errors introduce small deviations from the theoretical probability distribution. These deviations are limited by using integrators that leave the underlying "symplectic" structure of classical mechanics equations invariant. In this case the discretized equations actually solve the equations of motion corresponding to a so-called shadow Hamiltonian. A consequence is that also for long times the simulations errors (on average quantities) remain bounded. The most simple type of symplectic integrators are the second-order Verlet schemes. These schemes are highly efficient, and because of the favorable trade-off between accuracy and efficiency, they are commonly used. Also in the presence of constraints generalizations of these integrators have been proved to have the favorable symplectic properties (in the limit of full convergence of the equations that impose the constraints).[23]

So, the conservative part of the dynamics leaves the Boltzmann equation invariant (to good approximation), while the thermostatting leaves the canonical distribution invariant (exactly). During the conservative evolution the system remains on a constant energy hypersurface, while the thermostatting causes the energy to change. Therefore, if one is interested in sampling the canonical equilibrium distribution one can alternate purely conservative evolution with impulsive thermostatting.

**5.1. The Conservative Evolution.** For the conservative evolution we propose a velocity-Verlet type of implementation which produces (constrained) equal-time coordinates and velocities, as required for the thermostatting step. This implies the use of a RATTLE-type velocity constraining in addition to a SHAKE-type coordinate resetting. Here SHAKE and RATTLE do not refer to the iterative scheme used to impose the constraints—matrix methods may be used—but rather indicate that constraints are applied to positions only or also to velocities. In this case the conservative evolution can be computed as

$$\mathbf{v}_{n+1/2}(\lambda_n) \equiv \mathbf{v}_n + \frac{1}{2}\mathbf{M}^{-1}(\mathbf{f}_n + \sum_s \lambda_{ns}\nabla\sigma_s(\mathbf{x}_n))\Delta t \tag{50}$$

$$\mathbf{x}_{n+1}(\lambda_n) \equiv \mathbf{x}_n + \mathbf{v}_{n+1/2}(\lambda_n)\Delta t \tag{51}$$

$$\forall\ s\ \sigma_s(\mathbf{x}_{n+1}) = 0 \rightarrow \lambda_n \rightarrow \mathbf{x}_{n+1} \rightarrow \mathbf{v}_{n+1/2} \tag{52}$$

$$\mathbf{f}_{n+1} = -\nabla U(\mathbf{x}_{n+1}) \tag{53}$$

$$\mathbf{v}'_{n+1} = \mathbf{v}_{n+1/2} + \frac{1}{2}\mathbf{M}^{-1}\mathbf{f}_{n+1}\Delta t \tag{54}$$

$$\mathbf{v}_{n+1} = (\mathbf{I} - \mathbf{P})\mathbf{v}'_{n+1} \tag{55}$$

In this scheme the first two steps, eq 50 and eq 51, are formal because the Lagrange multipliers indicated by $\lambda_n$ are still unknown. In the constraining step given by eq 52 these Lagrange multipliers are computed and the conservative constraining forces and new positions are known. These can be used, together, with $\mathbf{f}_n$ to compute the virial contribution to the stress tensor. In the nomenclature of Section 4.2 the first three steps are realized by calling the routine xconstr eq 42 and then reconstructing the new midpoint velocities from the constrained positions:

$$\mathbf{x}_{n+1} = \text{xconstr}\left(\mathbf{x}_n + \mathbf{v}_n\Delta t + \frac{1}{2}\mathbf{M}^{-1}\mathbf{f}_n(\Delta t)^2;\ \mathbf{x}_n\right) \tag{56}$$

$$\mathbf{v}_{n+1/2} = (\mathbf{x}_{n+1} - \mathbf{x}_n)/\Delta t \tag{57}$$

The last two steps are realized by $\mathbf{v}_{n+1}$ = vconstr ($\mathbf{v}_{n+1/2}$ + $1/2\mathbf{M}^{-1}\mathbf{f}_{n+1}\Delta t$; $\mathbf{x}_{n+1}$).

In this scheme the midpoint velocity $\mathbf{v}_{n+1/2}$ is computed. Note that for this velocity $(\mathbf{I} - \mathbf{P})\mathbf{v}_{n+1/2} = O(\Delta t^2)$ and not exactly equal to zero. We also compute the velocities at integer number of time steps. These velocities are constrained such that $\mathbf{P}\mathbf{v}_{n+1} = 0$ exactly. The determination of fully constrained velocities at integer time steps is what distinguishes velocity-Verlet from Verlet or leapfrog schemes. This property is important for us because our thermostatting scheme, that can be applied next, uses the fact that the velocities are constrained. Note that this is different from Goga et al.[11] where leapfrog discretizations with a SHAKE-type constraining was used. In that work unconstrained thermostatting was applied to $\mathbf{v}_{n+1/2}$ and subsequently the updated positions were constrained. We now know that this procedure can give erroneous results if selected atoms or atom pairs are subjected to impulsive thermostatting.

For the Andersen and Lowe–Andersen thermostat the impulsive thermostat itself is discrete in nature. Its influence on the dynamics of a system is determined by the frequency the thermostat is applied and the number of particles (or pairs) that are actually thermostated. In other cases, like Langevin dynamics and DPD, the impulsive thermostat provides a discretization of an underlying stochastic differential equation (SDE). For these latter cases one might like to reproduce a dynamics that is as close as possible to the underlying dynamics of the SDE. In this case the time-step size dependence of dynamic quantities such as diffusivity and viscosity should be minimized.

**5.2. Implementation of the Thermostatting.** In our method, for the conservative part we need to constrain the position once and the velocity once. Next to that, for the thermostatting we need to compute velocity components perpendicular to the constrained space and at the end of the thermostatting constrain the velocities again. The basic operation is to project velocities (see Figure 3): either as as $\mathbf{v}^{\perp} = \mathbf{P}\mathbf{v}$ in eq 46, applied to the random vector $\mathbf{v} = \mathbf{M}^{-1/2}\boldsymbol{\xi}$, or as $\mathbf{v}^{c} = (\mathbf{I} - \mathbf{P})\mathbf{v}^{u}$ in eq 48, applied to the modified unconstrained velocities. These are simple operations once the routine vconstr eq 34 is available. The projection $\mathbf{P}$, for example, is computed by $\mathbf{v}^{\perp} = \mathbf{v} - \text{vconstr}(\mathbf{v};\mathbf{x}^{\text{ref}})$.

**5.3. Trotter Expansion.** The conservative Verlet or velocity-Verlet scheme discussed above is itself a second-order scheme with respect to the time step. This scheme can be symbolically written as VRV (velocity update, position update, velocity update).

If the impulsive thermostat follows from the discretization of a SDE, as for Langevin dynamics or DPD (but not for the Andersen and Lowe–Andersen thermostats), one might worry about the accuracy of the time discretization. For the dissipative and stochastic part of the SDEs the provided thermostatting scheme gives a first-order discretization for the dynamics (even though it leaves the equilibrium distribution invariant). This makes the total time evolution only first-order accurate.

Let us try to also make the discretization of the stochastic part second order. Note that, in practice, this is often not required. Langevin dynamics and DPD heavily influence the dynamics of a molecular system. This means that, if one is interested in short time transport coefficients, such as diffusion coefficients one will usually not use a thermostat based on this

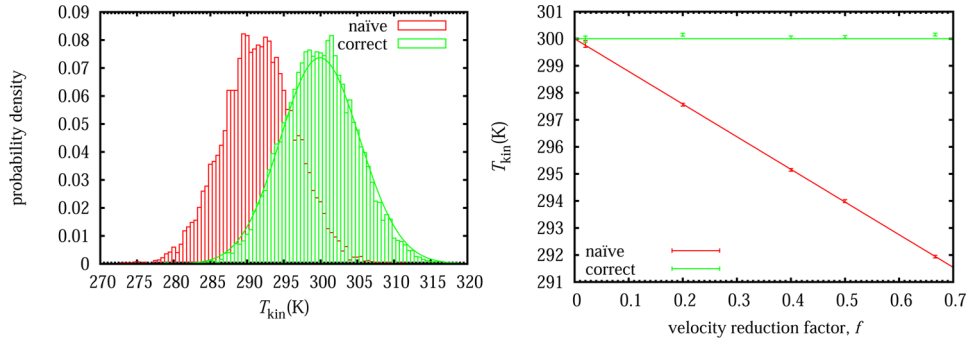


(a) histograms (b) $f$-dependence

**Figure 4.** Kinetic temperature is measured for a SPC/E-water simulation with an "iso-DPD" thermostat. The naïve thermostatting and the correct new thermostatting is applied. (a) The histogram for the two methods is compared for $f = 0.67$. The solid green line corresponds to the theoretically expected distribution. (b) The mean temperature is plotted as a function of $f$. For large values of $f$ the deviation from the thermostat temperature (300 K) is significant.

type of dynamics. The impulsive thermostat, however, already makes sure that the equilibrium distribution is invariant. Increasing its time accuracy does not improve this.

Having said this, let us assume that we need accurate stochastic dynamics. For an SDE we denote the stochastic dynamics as Ornstein−Uhlenbeck dynamics and denote it as "O". In Appendix A we discuss this dynamics, its analytical solution, and the construction of a Trotter expansion for the SDE. For unconstrained Langevin dynamics Leimkuhler and Matthews[24] have considered several second-order schemes constructed from Trotter expansion. They demonstrated that for Langevin dynamics VRORV performed best. For normal Langevin dynamics the analytical solution can be efficiently evaluated and does not have to be split up (see Appendix A). In other words all primitive thermostatting operations can be performed in parallel.

This is not the case SDEs that involve pair interaction, such as DPD. As shown in Appendix A in this case numerical evaluation of the Ornstein−Uhlenbeck dynamics is computationally very expensive. For an efficient evaluation of the Ornstein−Uhlenbeck dynamics the dynamics should be split up into individual pair-interactions. A second order Trotter scheme, where an individual primitive thermostat interaction corresponding to pair $k$ is $O_k$, gives $O \approx O_M \cdots O_2 O_1 O_2 \cdots O_M$. The need for a further Trotter expansion for the Ornstein−Uhlenbeck dynamics is discussed by Serrano et al.[13] and is also treated in Appendix A.

For the case where constraints are present for both Langevin and DPD dynamics the analytical solution for the O-dynamics can not be efficiently evaluated numerically. A Trotter expansion is possible in this case, see Appendix A.1. However, the price to pay is a large computational overhead because each of the individual primitive thermostatting operations involves a projection in this case (see Appendix B). We might follow the method introduced in this paper: of lifting the velocities from the constraint to the unconstraint manifold, next perform primitive thermostatting operations, and finally constrain the velocities. In this case the contrained Ornstein−Uhlenbeck dynamics is approximated as $O^c \approx LO_M \cdots O_2 O_1 O_2 \cdots O_M P$ (with L: lifting and P: projection). This is, however, not a true Trotter expansion and second order accuracy is not warranted.

Often, when discretization schemes for this type of dynamics are compared one looks at equilibrium quantities like the pair-distribution function (see, for example, ref 13). Note, however, that no difference will show up whether a Trotter expansion of first or second order is used for the O-dynamics, or whether a proper Trotter expansion for $O^c$ is used or the trick with lifting the velocities to the unconstraint manifold. The reason is that in any of these cases the equilibrium Boltzmann distribution is invariant. The only cause of deviation from equilibrium is the splitting of the conservative dynamics as into R and V. Therefore, one should consider transport properties such as diffusion coefficients to determine the improved time-step dependence of higher order schemes. Because we think the use of improved calculation of transport properties for stochastic dynamics is limited we did not implement the proper constrained second order Trotter expansion with its high computational overhead.

## 6. RESULTS

Two sets of results will be presented. First, we will repeat the simple analysis of a one-dimensional case discussed in Section 3. This will illustrate that indeed in this simple case the correct Maxwell−Boltzmann distribution is sampled. Second, we will show water simulations using the similar thermostats as in Goga et al.,[11] but with the improved thermostatting as discussed in Section 4.4.

**6.1. One-Dimensional Problem.** As a first illustration let us reconsider the first case in Section 3, depicted in Figure 1. With the new scheme the first step is to add thermal noise in the constrained directions. This noise of the relative velocity has variance $(k_B T/\mu)^{1/2}$ with $\mu = (1/2)m$. Next, the unconstrained thermostat is applied. Last, the constraining is applied:

$$v_1' = v_0 - \frac{1}{2}\sqrt{\frac{2k_B T}{m}}\xi_1,\ v_2' = v_0 + \frac{1}{2}\sqrt{\frac{2k_B T}{m}}\xi_1 \tag{58}$$

$$v_1'' = (1-f)v_1' + g\xi_2,\ v_2'' = v_2' \tag{59}$$

$$v_{cm} = \frac{1}{2}(v_1'' + v_2'') \tag{60}$$

The stationary variance can be computed by equating $\langle {v_{cm}}^2 \rangle = \langle {v_0}^2 \rangle$. To compute the value for $\langle {v_{cm}}^2 \rangle$ the properties of the Gaussian variables: $\langle {\xi_i}^2 \rangle = 1$, $\langle v_0\, \xi_i \rangle = 0$ and $\langle \xi_i \xi_j \rangle = 0$, for $i \neq j$ should be used. The value of $g$ is again related to $f$ by means of eq 3.

From this analysis we find that $\langle {v_{cm}}^2 \rangle = k_B T/2m$, which means that the computed kinetic temperature equals the


dx.doi.org/10.1021/ct500380x | J. Chem. Theory Comput. XXXX, XXX, XXX−XXX

Table 1. Diffusion Coefficients $[10^{-9}\ m^2/s]$ of Water at 298 K for Different Thermostatting Schemes

| $\tau_t$[ps] | ISO-1[a] | ISO-10[a] | ISO-20[a] | MD[b] | SD[c] |
|---|---|---|---|---|---|
| 1 | 2.622 ± 0.083 | 2.417 ± 0.028 | 2.160 ± 0.007 | 2.602 ± 0.246 | 2.352 ± 0.074 |
| 0.1 | 2.250 ± 0.153 | 1.181 ± 0.053 | 0.711 ± 0.002 | 2.493 ± 0.004 | 1.269 ± 0.024 |
| 0.01 | 1.092 ± 0.050 | 0.212 ± 0.013 | 0.146 ± 0.007 | 2.504 ± 0.087 | 0.202 ± 0.004 |
| 0.005 | 0.690 ± 0.001 | 0.147 ± 0.012 | 0.110 ± 0.000 | 2.542 ± 0.072 | 0.103 ± 0.001 |
| 0.004 | 0.560 ± 0.008 | 0.112 ± 0.011 | 0.107 ± 0.001 | 2.587 ± 0.007 | 0.079 ± 0.002 |

[a]ISO-$x$ is the iso-DPD thermostat with $x$ pair-interactions per particle. [b]MD: global Berendsen thermostat. [c]SD: stochastic Berendsen-van Gunsteren thermostat.

imposed temperature of the heat bath ($T_{kin} = T$). We leave it up to the reader to reexamine the second case discussed in Secton 3. Also in this case, as expected, the correct temperature is recovered.

**6.2. Water Simulations.** In this section we reexamine the constrained water simulations reported by Goga et al.[11] The temperature is examined for a simulation of 1024 water molecules using the SPC/E model[25] where all bond lengths and angles were constrained. A time step of $\Delta t = 2$ fs was used in all computations.

The thermostatting was performed with the isotropic DPD-like thermostat[11] where one pair per particle per time-step was chosen. The velocity update is as given by eq 23. Note, however, that the velocity reduction factor is position dependent. So in eq 23 substitute $f \rightarrow f \max(1 - r/r_c, 0)$, with a cutoff of $r_c = 1.2$ nm. This thermostat was implemented in both the "naïve" way, as outlined in Goga et al., and the "correct" way as outlined in the current paper. In Figure 4 results for the kinetic temperatures as a function of the $f$-factor are presented. When using the correct thermostatting procedure the measured kinetic temperature equals the one of the heat bath, that is, 300 K, whereas for the naïve implementation there is an erroneous large $f$-dependence.

In Table 1 a comparison of diffusion coefficients computed by different thermostats is presented. The parameter $\tau_t$ gives the relaxation time scale set in Gromacs.[26] For the iso-DPD thermostat the relation with the velocity reduction factor is $\tau_t = \Delta t/f$. For a global thermostat like the Berendsen thermostat the influence on the computed diffusion coefficient is little. The strength of the iso-DPD thermostat can be reduced by choosing as small $f$ (large $\tau_t$) and a small number of pair-interactions per particle. If the strength is small the diffusion coefficient is nearly unchanged. If the number of interactions is increased and/or $\tau_t$ is decreased the influence on the dynamics increases and the diffusion coefficient diminishes.

## 7. CONCLUSIONS AND DISCUSSION

In this paper we discussed the use of so-called impulsive thermostats in the presence of constraints. The most widely used impulsive thermostat is that of Andersen.[8] It is not widely acknowledged that, in the presence of constraints, this thermostat breaks down if only a limited number of atoms (instead of all) are re-equilibrated. This also occurs for other thermostats, such as Lowe–Andersen,[9] and impulsive implementations of DPD-type thermostats.[10,11]

We showed using a simple one-dimensional analysis that the problem is real and sometimes severe and we proposed a simple solution for it. This solution is to add velocity components in the constrained directions, next apply the impulsive thermostats to these unconstrained velocities and finally project the velocities back onto the constrained velocity space. This solution was demonstrated to resolve the issue for the simple one-dimensional cases as well as for water simulations previously presented.[11]

An implementation of a full DPD thermostat involving all pairs within a given range, will give rise to a substantial additional computational cost due to the large number of pairs that are subjected to friction and noise. If one is interested in applying accurate local thermostatting in a Galilean-invariant manner, but is not as much interested in full DPD dynamics, one might opt for the approach of Goga et al.,[11] who apply thermostatting to only one or a limited number of pairs per particle. In this way the extra overhead is minimized, while high-quality thermostatting is realized.

Using the impulsive schemes presented here, temperature deviations can only be caused by the conservative part of the equations of motion. We have advocated the use of the velocity-Verlet scheme, which uses a Trotter-splitting of the VRV type (where V is a conservative velocity update over $1/2\Delta t$ and R a coordinate update over $\Delta t$) and which is second-order accurate in $\Delta t$, combined with a single application of a sequence of primitive thermostatting operations to the velocities between two conservative steps. This amounts to an asymmetric VRVO scheme, where O is the impulsive velocity update over $\Delta t$. While the thermostatting is accurate and the overall scheme remains symplectic, the thermostatting will partly destroy the second-order precision in the dynamical evolution. It might be expected that symmetric impulsive schemes, such as RVOVR or OVRVO, have a higher dynamical accuracy, but this remains to be investigated. The addition of thermal noise deteriorates dynamical precision in any case. Properties that need to be addressed are the time-step dependence of quantities that depend on time correlations, like transport properties such as diffusivity and viscosity.

An issue, in this respect, is that the currently implemented impulsive thermostat with constraints can not be (fully) splitted as is needed for the Trotter expansion. In Appendix A.1 we present an implementation that can be splitted and is suited for Trotter expansion. However, this implementation will be computationally more expensive because many more projection steps need to be performed (see Appendix B). It remains to be investigated if in certain cases there is a benefit of using the more complicated version of rigorous impulsive constrained thermostatting.

## APPENDIX A. ORNSTEIN–UHLENBECK DYNAMICS

The full dynamics of a system evolving according to Langevin dynamics can be symbolically written as

$$\dot{\mathbf{z}} = \mathcal{L}\mathbf{z} = (\mathcal{L}_V + \mathcal{L}_R + \mathcal{L}_O)\mathbf{z} \tag{61}$$

where the state $\mathbf{z}$ denotes all particle positions and velocities. The formal solution is $\mathbf{z}(t) = \exp[\mathcal{L}t]\mathbf{z}(0)$. In a Trotter expansion the Liouvillian is split up into parts, and the solutions $\exp[\mathcal{L}_{sub}t]$ are used as building blocks of a numerical


dx.doi.org/10.1021/ct500380x | J. Chem. Theory Comput. XXXX, XXX, XXX–XXX

approximation. To be able to do this, clearly, the solution of the subdynamics corresponding to $\mathcal{L}_{\text{sub}}$ should be analytically solvable. This type of splitting for unconstrained ordinary Langevin equations has been considered, for example, by Bussi and Parrinello[27] and by Leimkuhler and Matthews.[24]

In eq 61 the Liouville operator corresponding to conservative velocity updates and position updates are

$$\mathcal{L}_{\mathbf{V}} = \mathbf{M}^{-1}\mathbf{f}\frac{\partial}{\partial \mathbf{v}}, \text{ and } \mathcal{L}_{\mathrm{R}} = \mathbf{v}\frac{\partial}{\partial \mathbf{r}} \tag{62}$$

If the mass matrix, $\mathbf{M}$, and the forces, $\mathbf{f}$, only depend on positions (and not on velocities) the time evolution corresponding to these sub-Liouvillians can be solved analytically to give

$$\dot{\mathbf{z}} = \mathcal{L}_{\mathrm{V}}\mathbf{z} \rightarrow \mathbf{v}(t) = \mathbf{v}(0) + \mathbf{M}^{-1}\mathbf{f}t,\ \mathbf{r}(t) = \mathbf{r}(0) \tag{63}$$

$$\dot{\mathbf{z}} = \mathcal{L}_{\mathrm{R}}\mathbf{z} \rightarrow \mathbf{v}(t) = \mathbf{v}(0),\ \mathbf{r}(t) = \mathbf{r}(0) + \mathbf{v}t \tag{64}$$

For example, the Trotter-expansion $\exp[(1/2)\mathcal{L}_{\mathrm{V}}\,\Delta t]\exp[\mathcal{L}_{R}\,\Delta t]\exp[(1/2)\mathcal{L}_{\mathrm{V}}\,\Delta t]$ corresponds to the velocity-Verlet algorithm. In the main text we indicate this scheme as VRV.

The dynamics of the Ornstein−Uhlenbeck part of the Langevin dynamics, $\mathcal{L}_O$, corresponds to the stochastic differential equation

$$\mathbf{M}\mathrm{d}\mathbf{v} = -\boldsymbol{\gamma}\mathbf{v}\mathrm{d}t + \sqrt{2k_{\mathrm{B}}T\boldsymbol{\gamma}}\,\mathrm{d}\mathbf{W}_t,\ \mathrm{d}\mathbf{x} = \mathbf{0} \tag{65}$$

where each component of the vector $\mathbf{W}_t$ is a Wiener process. If the mass matrix, $\mathbf{M}$, and the friction matrix, $\boldsymbol{\gamma}$, only have a positional dependence the analytical solution is

$$\begin{aligned}\mathbf{v}(t) &= \exp[-\mathbf{M}^{-1}\boldsymbol{\gamma}t]\mathbf{v}(0)\\ &\quad + \sqrt{k_{\mathrm{B}}T(\mathbf{I} - \exp[-2\mathbf{M}^{-1}\boldsymbol{\gamma}t])\mathbf{M}^{-1}}\,\boldsymbol{\xi},\\ \mathbf{x}(t) &= \mathbf{x}(0)\end{aligned} \tag{66}$$

Here $\boldsymbol{\xi}$ is a vector of independent Gaussian variables each with mean 0 and variance 1. In terms of the update scheme given by eq 18 we find that

$$\begin{aligned}\mathbf{F} &= \mathbf{I} - \exp[-\mathbf{M}^{-1}\boldsymbol{\gamma}t] \text{ and } \mathbf{G}\\ &= \sqrt{k_{\mathrm{B}}T(\mathbf{I} - \exp[-2\mathbf{M}^{-1}\boldsymbol{\gamma}t])\mathbf{M}^{-1}}\end{aligned} \tag{67}$$

Because these matrices obey eq 20 the update leaves the Maxwell−Boltzmann distribution invariant (as it should).

For ordinary Langevin dynamics the mass matrix $\mathbf{M}$ and the friction matrix $\boldsymbol{\gamma}$ are diagonal (and possible position dependent). In this case the rigorous solution can be easily computed. This is different in the case where these matrices are nondiagonal, but remain sparse. Still, in this case the solution can be computed numerically, but computing the exponents (and square-root) of the matrices is computationally demanding. This can be probably achieved by applying Krylov subspace methods such as implemented in Expokit.[28]

To avoid this expensive computation, but still retain valuable properties one can try to decompose $\mathcal{L}_O$ further in sub-Liouvillians that can be solved analytically. To obtain a second-order Trotter expansion we can split-off one sub-Liouvillian at a time. If we define $\mathcal{L}_{r-O}^{(k)}$ as the remaining Ornstein−Uhlenbeck operator with $k$ sub-Liouvillians split of we find, recursively, for a second order expansion,

$$\exp[\mathcal{L}_{r-O}^{(k)}t] \approx \exp\left[\frac{1}{2}\mathcal{L}_O^{(k)}t\right]\exp[\mathcal{L}_{r-O}^{(k+1)}t]\exp\left[\frac{1}{2}\mathcal{L}_O^{(k)}t\right] \tag{68}$$

where $\mathcal{L}_{r-O}^{(0)} = \mathcal{L}_O$ and $\mathcal{L}_{r-O}^{(3M)} = 0$.

If we continue up to the point that all Ornstein−Uhlenbeck sub-Liouvillians are split we find sequence of changes of velocities of each pair according to eq 66. So, in symbolic notation we have $O \approx O_{3M}...O_2O_1O_1O_2...O_{3M}$. Note that we find that the final result will be different depending on the numbering of the pairs. However, any of these alternatives is a valid second-order expansion.

A way to split up the Ornstein−Uhlenbeck Liouville operator is to decompose the friction matrix as

$$\boldsymbol{\gamma} = \sum_k \boldsymbol{\gamma}_k \text{ with } \boldsymbol{\gamma}_k = \nu_k\mathbf{u}_k\mathbf{u}_k^T \text{ and } \mathbf{u}_k^T\mathbf{M}^{-1}\mathbf{u} = 1. \tag{69}$$

In this case each subfriction matrix has rank 1. The normalization of $\mathbf{u}$ is such that the matrix exponential in eq 67 (with $\boldsymbol{\gamma} \rightarrow \boldsymbol{\gamma}_k$) can be easily evaluated. For $\boldsymbol{\gamma}_k$ eq 67 reduces to eq 29, which is an expression that can be easily evaluated numerically.

This situation of a nondiagonal friction matrix typically arises in the case of DPD dynamics. In this case the Ornstein−Uhlenbeck dynamics is

$$m_i\mathrm{d}\mathbf{v}_i = -\sum_j \gamma\mathbf{f}(r_{ij})(\mathbf{v}_i - \mathbf{v}_j) + \sum_{j\neq i}\sqrt{2k_{\mathrm{B}}T\gamma\mathbf{f}(r_{ij})}\,\mathrm{d}\mathbf{W}_{ij} \tag{70}$$

In this equation the boldface indicates the three spatial directions and the subscripts correspond to particle indices. So, we can imagine the big matrix $\boldsymbol{\gamma}$ as in eq 65 to consist of $3 \times 3$ blocks with values of $-\gamma f(r_{ij})$ on the $ij$ off-diagonal block and of $\gamma\sum_{j\neq i}\mathbf{f}(r_{ij})$ on the diagonal $ii$-block. The mass matrix is diagonal. In this formula there is one independent Wiener process for each pair (in each spatial direction), and $\mathbf{W}_{ij} = -\mathbf{W}_{ji}$ (such that momentum is conserved).

Instead of computing complicated matrix functions we further subdivide $\mathcal{L}_O$ by considering each pair interaction separately. If we denote $\mathcal{L}_O^{(k)}$ as the Liouvillian corresponding to pair the pair indicated by the label $k$ (say $k$ corresponds to the pair $ij$). Then $\mathcal{L}_O = \sum_k\mathcal{L}_O^{(k)}$, that is, the sum over all pairs. In that case an $\mathcal{L}_O^{(k)}$ would correspond to the dynamics

$$m_i\mathrm{d}\mathbf{v}_i = -\gamma\mathbf{f}(r_{ij})(\mathbf{v}_i - \mathbf{v}_j) + \sqrt{2k_{\mathrm{B}}T\gamma\mathbf{f}(r_{ij})}\,\mathrm{d}\mathbf{W}_k \tag{71}$$

$$m_j\mathrm{d}\mathbf{v}_j = -\gamma\mathbf{f}(r_{ij})(\mathbf{v}_j - \mathbf{v}_i) - \sqrt{2k_{\mathrm{B}}T\gamma\mathbf{f}(r_{ij})}\,\mathrm{d}\mathbf{W}_k \tag{72}$$

This system has the same shape as eq 65 only in this case the matrix $\gamma$ only has nonzero entries for the $3 \times 3$ blocks corresponding particles $i$ and $j$.

The only potential issue is that the $3 \times 3$ matrix $\mathbf{f}(r_{ij})$ might need to be decomposed. Usually, however, its shape is either isotropic $\mathbf{f}(r_{ij}) = f_{\text{iso}}(r_{ij})\mathbf{I}$ or anisotropic of the form $\mathbf{f}(r_{ij}) = f_{\parallel}(r_{ij})\,\hat{\mathbf{r}}_{ij}\hat{\mathbf{r}}_{ij}^T + f_{\perp}(r_{ij})\,(\mathbf{I}-\hat{\mathbf{r}}_{ij}\hat{\mathbf{r}}_{ij}^T)$. In both cases the matrix is already effectively diagonal and the computation of matrix functions is trivial. To cleanly connect to the *primitive thermostatting operations* we can consider the three spatial directions separately. If we do this then every index $k$ indicates a pair and direction combination. Thus, if there are $M$ pairs the index $k$ runs from 1 to $3M$. Note that in the usual case of DPD, the primitive operations in the three directions can be applied in parallel without causing issues.


dx.doi.org/10.1021/ct500380x | J. Chem. Theory Comput. XXXX, XXX, XXX−XXX

As a concrete example let us consider the primitive thermostatting operation between particles 1 and 2 in the parallel direction for anisotropic DPD. In that case

$$\mathbf{u} = \sqrt{\mu}\begin{pmatrix}\hat{\mathbf{r}}_{12}\\ -\hat{\mathbf{r}}_{12}\end{pmatrix}, \text{ and } \nu = (\gamma/\mu) f_{\parallel}(r_{12}) \tag{73}$$

Here the reduced mass, $\mu$, occurs to ensure that $\mathbf{u}^T\mathbf{M}^{-1}\mathbf{u} = 1$. According to the analytical solution, eq 29, the analytical primitive thermostat operation is thus characterized by

$$\mathbf{F} = (1 - \exp(-\nu\Delta t))\begin{pmatrix}(\mu/m_1)\hat{\mathbf{r}}_{12}\hat{\mathbf{r}}_{12}^T & -(\mu/m_1)\hat{\mathbf{r}}_{12}\hat{\mathbf{r}}_{12}^T\\ -(\mu/m_2)\hat{\mathbf{r}}_{12}\hat{\mathbf{r}}_{12}^T & (\mu/m_1)\hat{\mathbf{r}}_{12}\hat{\mathbf{r}}_{12}^T\end{pmatrix} \tag{74}$$

$$\mathbf{g} = \sqrt{\mu k_B T(1 - \exp(-2\nu\Delta t))}\begin{pmatrix}\hat{\mathbf{r}}_{12}/m_1\\ -\hat{\mathbf{r}}_{12}/m_2\end{pmatrix} \tag{75}$$

**A.1. Constrained Ornstein–Uhlenbeck Dynamics.** If we apply constraints the Ornstein–Uhlenbeck dynamics changes to

$$\mathbf{M}d\mathbf{v} = -\boldsymbol{\gamma}\mathbf{v}dt + \sqrt{k_B T\boldsymbol{\gamma}}\,d\mathbf{W}_t - \mathbf{C}^T d\lambda,\ d\mathbf{x} = \mathbf{0} \tag{76}$$

where $d\lambda$ is such that $\mathbf{C}\mathbf{v} = \mathbf{0}$. This gives

$$\mathbf{M}d\mathbf{v} = -\boldsymbol{\gamma}^c\mathbf{v}dt + \sqrt{k_B T\boldsymbol{\gamma}^c}\,d\mathbf{W}_t \text{ with } \boldsymbol{\gamma}^c = (\mathbf{I} - \mathbf{P})^T\boldsymbol{\gamma}(\mathbf{I} - \mathbf{P}) \tag{77}$$

If we derive the decomposition for the constrained case from the unconstrained one, that is, take $\boldsymbol{\gamma}_k^c = (\mathbf{I} - \mathbf{P})^T\boldsymbol{\gamma}_k(\mathbf{I} - \mathbf{P})$, we find with $\boldsymbol{\gamma}_k^c = \nu_k^c\mathbf{u}_k^c\mathbf{u}_k^{c,T}$

$$\nu_k^c = (\mathbf{u}_k^T(\mathbf{I} - \mathbf{P})\mathbf{M}^{-1}\mathbf{u}_k)\nu_k \text{ and } \mathbf{u}_k^c = \frac{(\mathbf{I} - \mathbf{P}^T)\mathbf{u}_k}{\sqrt{\mathbf{u}_k^T(\mathbf{I} - \mathbf{P})\mathbf{M}^{-1}\mathbf{u}_k}} \tag{78}$$

With these definitions the analytical solution again follows from eq 29. Note that, when constructing $\mathbf{u}_k^c$ from $\mathbf{u}_k$, a factor is introduced that ensures $\mathbf{u}_k^{c,T}\mathbf{M}^{-1}\mathbf{u}_k^c = 1$. While in the solution of, for example, the DPD equations $\mathbf{u}_k$ has two nonzero entries, namely, for the two particles in pair $k$, the projection makes that $\mathbf{u}_k^c$ all particles connected by constrains to either of these particles are involved. This issue will be discussed in a more general setting below.

## APPENDIX B. PRIMITIVE ONE-STEP OPERATIONS FOR CONSTRAINED IMPULSIVE THERMOSTATTING

Suppose we would like to produce correct impulsive thermostatting in the presence of constraints without the need of (temporary) introducing velocity components in unconstrained directions. Let us write such a scheme for a primitive (one-dimensional) thermostatting operation again (cf. eq 21) as

$$\mathbf{v}' = (\mathbf{I} - \mathbf{F}^c)\mathbf{v} + \mathbf{g}^c\xi \tag{79}$$

but now keeping both $\mathbf{F}^c\mathbf{v}$ and $\mathbf{g}^c$ within the constraint hyperspace. This implies that $\mathbf{P}\mathbf{F}^c\mathbf{v} = \mathbf{P}^c\mathbf{g}^c = \mathbf{0}$. In this case the covariance matrix should correspond to the constrained canonical distribution eq 43, such that

$$k_B T(\mathbf{I} - \mathbf{P})\mathbf{M}^{-1} = k_B T(\mathbf{I} - \mathbf{F}^c)(\mathbf{I} - \mathbf{P})\mathbf{M}^{-1}(\mathbf{I} - \mathbf{F}^{c,T}) + \mathbf{g}^c\mathbf{g}^{c,T} \tag{80}$$

which can be rewritten as (cf. eq 22)

$$\mathbf{g}^c\mathbf{g}^{c,T} = k_B T[\mathbf{F}^c(\mathbf{I} - \mathbf{P})\mathbf{M}^{-1} + (\mathbf{I} - \mathbf{P})\mathbf{M}^{-1}\mathbf{F}^{c,T} - \mathbf{F}^c(\mathbf{I} - \mathbf{P})\mathbf{M}^{-1}\mathbf{F}^{c,T}] \tag{81}$$

A primitive operation that obeys this relation is, similar to eq 22,

$$\mathbf{F}^c = f\frac{\mathbf{g}^c\mathbf{g}^{c,T}\mathbf{M}}{\mathbf{g}^{c,T}\mathbf{M}\mathbf{g}^c}, \text{ with } f(2 - f) = \frac{\mathbf{g}^{c,T}\mathbf{M}\mathbf{g}^c}{k_B T} \tag{82}$$

but under the extra condition that $\mathbf{P}\mathbf{g}^c = \mathbf{0}$. This condition implies that $\mathbf{P}\mathbf{F}^c = \mathbf{0}$. It is satisfied if $\mathbf{g}^c$ is constructed from an unconstrained vector $\mathbf{g}$ as

$$\mathbf{g}^c = (\mathbf{I} - \mathbf{P})\mathbf{g} \tag{83}$$

Equation 82 is very analogous to the one given in eq 25. Its validity can be checked by back-substitution in eq 81 and using the identities given in eq 45.

In practice one may proceed as follows: First construct a vector $\mathbf{g}$ as in an unconstrained case, for example, as given in eq 24 for the one-dimensional *iso*-DPD example. Next, apply the vconstr($\mathbf{g}$) routine to construct $\mathbf{g}^c$, followed by a construction of $\mathbf{F}^c$ according to eq 82. Note that, although projection of the unconstrained $\mathbf{g}$ gives a result that leaves the constrained Maxwell–Boltzmann invariant, if one wants to construct a analytical solution of constrained Ornstein–Uhlenbeck dynamics then substituting eq 78 into eq 29 gives that there is an extra time-step dependent factor involved. Also note that this projection step mixes all components that are related to the thermostated pair through (a sequence of) constraints, thus loosing the simplicity of the unconstrained thermostatting event.

Sequential application of these primitive operations gives rise to the constrained canonical distribution. This is achieved without leaving the constraint hypersurface. Each individual primitive operation leaves the constrained canonical distribution invariant. Therefore, these operations, actually the one that follows from eq 78, can be used in a splitting scheme such as a higher order Trotter expansion.

The main drawback of this method is that for the computation of each $\mathbf{g}_k^c$ in a sequence of primitive thermostatting operations a projection is needed. It depends on the molecular system that is being simulated if this is in fact expensive or not. In general, only one or two particle velocities would be influenced by the unprojected primitive vector $\mathbf{g}$. The constraints, however, create a connected path. If the particles are "connected" by means of constraints to many other particles then many velocities need to be updated during the application of friction and noise.

So in general, if the connectedness is relatively small as in a water simulation, the extra overhead will be limited. If, however, the connectedness is large, such as in macromolecule simulations where all bond lengths and angles are constrained, the overhead of this scheme compared to the one discussed in the main body will be huge.

## AUTHOR INFORMATION

**Corresponding Author**

*E-mail: e.a.j.f.peters@tue.nl.

## Notes

The authors declare no competing financial interest.

## REFERENCES


(1) Ermak, D. L.; Buckholz, H. *J. Comput. Phys.* **1980**, *35*, 169−182.
(2) Allen, M. P.; Tildesley, D. J. *Computer Simulation of Liquids;* Oxford University Press: New York, 1989.
(3) Frenkel,D.; Smit, B. *Understanding Molecular Simulation,* 2nd ed.; Prentice Hall: New Jersey, 2001.
(4) Berendsen, H. J. C. *Simulating the Physical World, A Hierarchy of Models for Simulation;* Cambridge University Press: Cambridge, U.K., 2007.
(5) Van Gunsteren, W. F.; Berendsen, H. J. C.; Rullmann, J. A. C. *Mol. Phys.* **1981**, *44*, 69−95.
(6) Van Gunsteren, W. F.; Berendsen, H. J. C. *Mol. Phys.* **1982**, *45*, 637−647.
(7) Van Gunsteren, W. F.; Berendsen, H. J. C. *Mol. Simul.* **1988**, *1*, 173−185.
(8) Andersen, H. C. *J. Chem. Phys.* **1980**, *72*, 2384−2393.
(9) Lowe, C. P. *Europhys. Lett.* **1999**, *47*, 145−151.
(10) Peters, E. A. F. J. *Europhys. Lett.* **2004**, *66*, 311−317.
(11) Goga, N.; Rzepiela, A. J.; de Vries, A. H.; Marrink, S. J.; Berendsen, H. J. C. *J. Chem. Theory Comput.* **2012**, *8*, 3637−3649.
(12) Sivak, D. A.; Chodera, J. D.; Crooks, G. E. *arXiv:1301.3800v2 [physics.comp-ph]* **2013**, 1−15.
(13) Serrano, M.; De Fabritiis, G.; Español, P.; Coveney, P. V. *Math. Comput. Simul.* **2006**, *72*, 190−194.
(14) Ryckaert, J.-P.; Ciccotti, G. *Mol. Phys.* **1986**, *58*, 1125−1136.
(15) Vanden Eijnden, E.; Ciccotti, G. *Chem. Phys. Lett.* **2006**, *429*, 310−316.
(16) Kallemov, B.; Miller, G. H. *SIAM J. Sci. Comput.* **2011**, *33*, 653−676.
(17) Koelman, J. M. V. A.; Hoogerbrugge, P. J. *Europhys. Lett.* **1993**, *21*, 363−368.
(18) Shardlow, T. *SIAM J. Sci. Comput.* **2003**, *24*, 1267−1282.
(19) Ryckaert, J. P.; Ciccotti, G.; Berendsen, H. J. C. *J. Comput. Phys.* **1977**, *23*, 327−341.
(20) Miyamoto, S.; Kollman, P.A. *J. Comput. Chem.* **1992**, *13*, 952−962.
(21) Hess, B.; Bekker, H.; Berendsen, H. J. C.; Fraaije, J. G. E. M. *J. Comput. Chem.* **1997**, *18*, 1463−1472.
(22) Hess, B. *J. Chem. Theory Comput.* **2008**, *4*, 116−122.
(23) Leimkuhler, B. J.; Skeel, R. D. *J. Comput. Phys.* **1994**, *112*, 117−125.
(24) Leimkuhler, B.; Matthews, C. *Appl. Math. Res. Express* **2013**, *1*, 34−56.
(25) Berendsen, H. J. C.; Grigera, J. R.; Straatsma, T. P. *J. Phys. Chem.* **1987**, *91*, 6269−6271.
(26) van der Spoel, D.; Lindahl, E.; Hess, B.; van Buuren, A. R.; Apol, E.; Meulenhoff, P. J.; Tieleman, D. P.; Sijbers, A. L. T. M.; Feenstra, K. A.; van Drunen R.; Berendsen, H. J. C. *Gromacs User Manual, Version 4.5.6;* 2010. http://www.gromacs.org (accessed July 1, 2014).
(27) Bussi, G.; Parrinello, M. *Phys. Rev. E* **2007**, *75*, 056707.
(28) Sidje, R. B. *ACM Trans. Math. Software* **1998**, *24*, 130−156.